engineering proceedings

MDPI

Proceeding Paper

Innovative Plasmonic Sensors Based on Plastic Optical Fibers, Optical Adhesives and Thin Films †

Chiara Marzano *, Francesco Arcadio, Luigi Zeni, Domenico Del Prete and Nunzio Cennamo *

Department of Engineering, University of Campania Luigi Vanvitelli, Via Roma 29, 81031 Aversa, Italy; francesco.arcadio@unicampania.it (F.A.); luigi.zeni@unicampania.it (L.Z.); domenico.delprete@unicampania.it (D.D.P.)

* Correspondence: chiara.marzano@studenti.unicampania.it (C.M.); nunzio.cennamo@unicampania.it (N.C.); Tel.: +39-0815010367

† Presented at the 4th International Electronic Conference on Applied Sciences, 27 October–10 November 2023; Available online: https://asec2023.sciforum.net/.

Abstract: Plasmonic phenomena can be used to realize sensors and biosensors in several application fields. This work presents polymer-based plasmonic sensor chips made by simple and cheap realization steps. The proposed sensors are small-size, highly sensitive, versatile, low-cost, and useful to realize disposable biosensors. In detail, to realize these sensors, a resin block with a custom-shaped trench inside is achieved by a 3D printer. This trench is filled with a UV-cured optical adhesive to achieve the core of a multimode optical waveguide when the end of the trench is closed by two plastic optical fiber (POF) patches. Then, a photoresist buffer layer is deposited by spinning on the optical waveguide, and finally, a gold nanofilm is sputtered to excite the plasmonic phenomenon. The buffer layer improves the sensor performance and the gold's adhesion on the surface. The optical waveguide's shape can be changed to match the sensor chip with different experimental setups, such as the one based on the smartphone's CCD camera and LED. In this way, receptor layers can be deposited on the highly sensitive gold surface to realize high-performance bio/chemical sensors for several application fields, such as Point-Of-Care Tests (POCT) and environmental monitoring.

Keywords: optical sensors; surface plasmon resonance (SPR); plastic optical fibers (POFs); optical adhesives

Citation: Marzano, C.; Arcadio, F.; Zeni, L.; Del Prete, D.; Cennamo, N. Innovative Plasmonic Sensors Based on Plastic Optical Fibers, Optical Adhesives and Thin Films. *Eng. Proc.* **2023**, *52*, x. https://doi.org/10.3390/xxxxx

Academic Editor(s): Name

Published: date

1. Introduction

Surface plasmon resonance (SPR) is a physical phenomenon that measures refractive index variations present at the interface between a dielectric medium and metal nanofilms [1–3].

Polymer-based SPR sensors are typically chosen over glass-based sensors within the class of optical waveguide-based plasmonic sensors because they have several advantages, including flexibility, ease of handling, low cost, and a straightforward manufacturing procedure.

Modern 3D printing technologies have significantly accelerated the creation of cutting-edge sensors. Among the main advantages of using 3D printing technology is the ability to create more complex geometries than normal cylindrical fibers. On this line, Cennamo et al. recently built innovative SPR sensors using a low-cost strategy based on 3D inkjet printing technology coupled with photoactive resins [4].

The SPR sensor performance can be changed by exploiting the shape and the size of the 3D-printed trench and/or by changing the refractive index of the optical adhesive (core). For instance, this work presents three different 3D-printed SPR sensors made of light-curing resins using a similar method reported in [4]. In order to explore the impact of the refractive index of the core (the kind of resin) on the plasmonic performance, the

resins (which constitute the core of the waveguides) in 3D-printed support have been changed [5]. Specifically, three sensor configurations with core refractive indices of 1.48, 1.50, and 1.54 were optically analyzed and compared.

2. Plasmonic Sensor Systems

2.1. Sensor's production steps

Based on different core refractive indices (different resins), the three sensor configurations are made by the production process reported in [5]. This simple production process is recalled in the following paragraph.

In the first phase, support had to be built to host the waveguide's core of the three different sensor configurations; this support was designed through commercial software [5]. Figure 1 depicts schematic cross-sections illustrating its dimensions. These SPR sensor configurations are studied to test the performance against an SPR platform based on a modified plastic optical fiber (POF) [6].

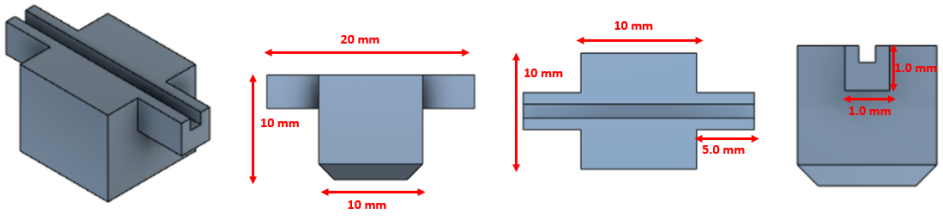

Figure 1. Outline of the 3D printed support with the trench to be filled with different UV optical adhesives [5].

The above-described holders are printed via a 3D printer using a UV-sensitive grey resin (more details are reported in [5]).

Once the supports were ready, two POF patches were inserted at the two ends of the trench in order to connect the light source and the spectrometer with the sensing region. Then, a first layer of UV-cured optical adhesive is poured inside the trench. The platforms were then polymerized for about 10 min using a lamp bulb [5].

The optical adhesive was discovered to have considerable shrinkage after the UV curing of the first layer, resulting in a smaller core size than was originally intended [5].

When working with plasmonic sensors based on optical waveguides, the core size is closely related to the multimodality property of waveguides, which is a key feature to characterize plasmonic performance [7]. Hence, the waveguide with a core thickness of 1 mm was created by a second jet of optical adhesive [5]. After being polymerized for 10 *min*, the three sensor configurations are exposed to a lapping procedure utilizing first a paper with a grain size of 5 µm and successively 1 µm (similarly to [6]). After that, a buffer layer of photoresist (1.5 µm tick) is spin-coated to improve the sensor's plasmonic performance thanks to its high refractive index (1.61) [5,6]. In addition, this buffer layer helps the adhesion between the optical adhesive layer and the subsequent gold layer. Finally, a sputter coater machine is utilized to deposit a nanolayer (about 60 nm) of gold on the sensitive region in order to ensure the fulfillment of the surface plasmon resonance principles.

More details about the manufacturing technologies used to produce this kind of plasmonic sensors are reported in [5].

Figure 2 shows a view from above and in the section of the proposed platforms [5], which are named as reported below: "Configuration 1", having a refractive index of the 1.48; "Configuration 2" of 1.50; and "Configuration 3" of 1.54.

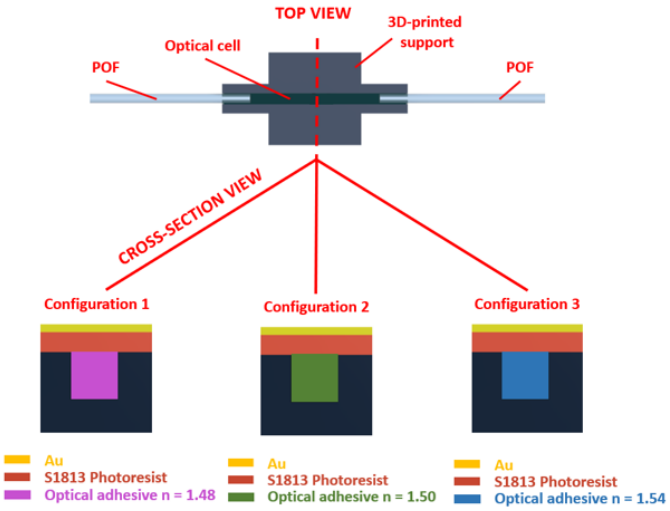

Figure 2. SPR sensors outline carried out by a different core refractive index [5].

2.2. Experimental setup

The three sensor configurations are characterized by an optical point of view using the following experimental setup [5]. As reported in Figure 3, a spectrophotometer and a white light source are connected with the sensing chip reported in Figure 2 exploiting its POFs. In other words, the light was launched into the optical adhesive (waveguide core) and collected at the exit using the two POF patches fixed at the ends of the trench. SMA connectors are used to make the various connections. A computer is connected to the spectrophotometer in order to collect and process the experimental data.

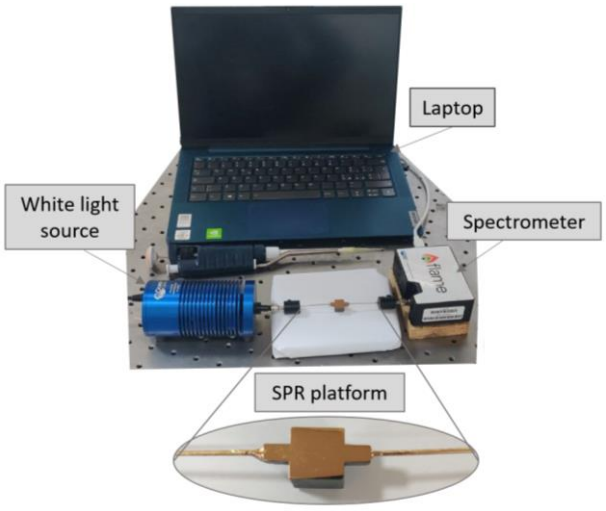

Figure 3. Picture of the experimental setup used to test the SPR sensors [5].

Solutions made by combining water and glycerin ranging in refractive index from 1.332 RIU to 1.384 RIU are used to obtain an optical characterization [5]. Each solution is examined before use by an Abbe refractometer.

3. Results and Discussion

Figure 4 displays the SPR spectra achieved for each sensor configuration at several solutions with different refractive indices [5].

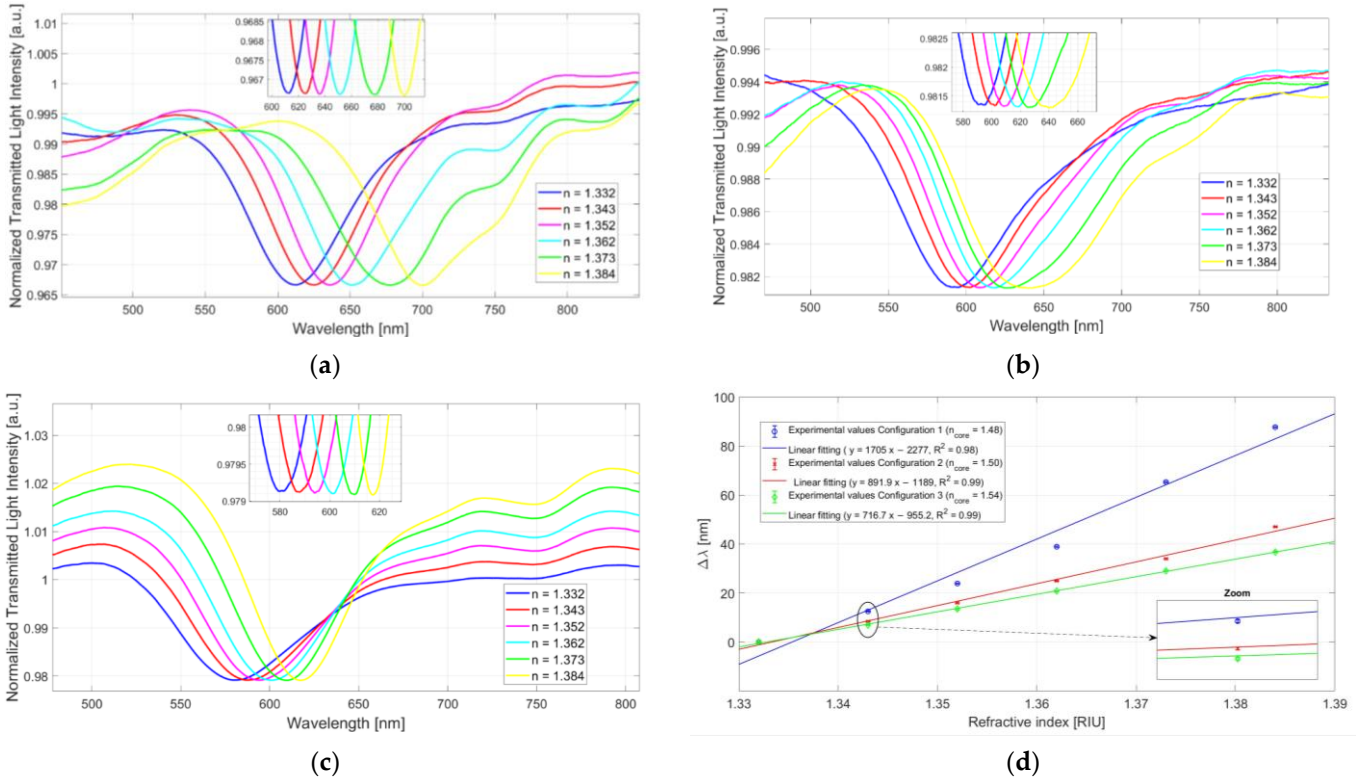

Figure 4. SPR spectra at several refractive indices for sensors based on a different core refractive index: (**a**) of 1.48 RIU, (**b**) of 1.50 RIU, and (**c**) of 1.54 RIU. (**d**) Variation of the resonance wavelength with respect to the refractive indices of the external solutions and linear fitting of the experimental data for the three tested configurations [5].

The optical characterization of the three platforms was done in terms of sensitivity and resolution.

The bulk sensitivity (S) is determined as the variation of the resonance wavelength ($\delta\lambda_{res}$) per unit change in refractive index (δn_s). Therefore, the bulk sensitivity is defined as follows [5,6,8]:

$$S = \left(\frac{\delta\lambda_{res}}{\delta n_s}\right)_{n_s} \quad \left[\frac{nm}{RIU}\right] \tag{1}$$

Concerning the resolution (Δn), it is defined as the minimum variation of the refractive index appreciable by the sensor system and is calculated as follows [5,6,8]:

$$\Delta n = \frac{\delta n_s}{\delta\lambda_{res}}\delta M = \frac{1}{S}\,\delta M \quad [RIU] \tag{2}$$

where δM is the standard deviation of the resonance wavelength, and it depends on the spectral resolution of the used spectrometer.

As seen in Figure 4a–c, when the solution's refractive index on the sensitive surface increases, the resonance wavelength is shifted to higher values (red-shift) for each configuration [5].

Figure 4d shows the resonance wavelength shift versus the solution's refractive index for each configuration tested [5]. A linear function fitted the experimental data achieved for every configuration to carry out a first-order analysis.

These fittings show a good R^2 value for all analyzed configurations. In particular, this parameter is 0.98 for the platform with a core refractive index of 1.48 and 0.99 for the platforms with a refractive index of the core of 1.50 and 1.54.

Each experimental data reported in Figure 4d is the mean of three successive measurements, and the respective standard deviations are reported as error bars [5].

The bulk sensitivity (Equation (1)) has been approximated as the slope of the linear fitting function, and the resolution in terms of the lowest observable change in refractive index can be approximated as reported in Equation (2). The obtained sensor parameters are summarized in Table 1 [5].

Table 1. Comparative analysis of the three sensors realized and tested [5].

$\mathbf{n_{core}}$ [RIU]	S $\left[\frac{nm}{RIU}\right]$	Δn [RIU]	R^2
1.48	1705	0.88×10^{-3}	0.98
1.50	892	1.68×10^{-3}	0.99
1.54	717	2.09×10^{-3}	0.99

As can be seen from Table 1, the best plasmonic performances are obtained by exploiting a core with a refractive index of 1.48.

Therefore, as evidenced by a similar approach in [9], the sensitivity increases with the reduction of the core refractive index.

Moreover, Figure 4a–c clearly show that the SPR curve's width decreases as the core's refractive index increases. This feature is due to the fact that, compared to Configuration 1, Configuration 2, and Configuration 3, fewer higher-order modes (which are the most sensitive) satisfy the SPR condition [5].

Finally, it can be noticed that the performances obtained by the better sensor configuration are very close to those achieved by an SPR D-shaped POF sensor (based on a core of PMMA, whose refractive index is 1.49) [6].

4. Conclusions

A comparative analysis of three SPR sensors having the same size and geometry but different core refractive indices found that the configuration with better optical performance, in terms of sensitivity and resolution, has a core refractive index of 1.48, as best reported in [5].

Future developments could see the best proposed SPR sensor configuration protagonist to realize bio/chemical chips with disposable and low-cost characteristics. In addition, the further advantage of the described approach is obtaining waveguides whose channels can have various shapes. Tuning different shapes could be useful to have the light source and the receiver on the same side, making it possible to test the platform using the Light Emitting Diode (LED) and the Charge Coupled Device (CCD) of the smartphone to carry out bio/chemical tests independently and quickly [10–13].

Author Contributions: Conceptualization, F.A., C.M., D.D.P., N.C. and L.Z.; methodology, F.A., C.M., D.D.P., N.C. and L.Z.; validation, F.A., C.M., D.D.P., N.C. and L.Z.; formal analysis, F.A., C.M., D.D.P., N.C. and L.Z.; investigation, F.A., C.M., D.D.P., N.C. and L.Z.; resources, N.C. and L.Z.; data curation, F.A., C.M., D.D.P., N.C. and L.Z.; writing—original draft preparation, F.A., C.M., D.D.P., N.C. and L.Z.; writing—review and editing, F.A., C.M., D.D.P., N.C. and L.Z.; supervision, L.Z. and N.C. All authors have read and agreed to the published version of the manuscript.

Funding: This research received no external funding.

Institutional Review Board Statement: Not applicable.

Informed Consent Statement: Not applicable.

Data Availability Statement: The data are available on reasonable request from the corresponding author.

Acknowledgments: The authors acknowledge the Regione Campania for the BETTER Project–POR FESR CAMPANIA 2014-2020 program.

Conflicts of Interest: The authors declare no conflict of interest.

References

1. Tong, R.-J.; Wang, Y.; Zhao, K.-J.; Zhao, Y. Surface Plasmon Resonance Optical Fiber Sensor for Refractive Index Detection Without Temperature Crosstalk. *IEEE Trans. Instrum. Meas.* **2022**, *71*, 7002806.
2. Li, L.; Zhang, Y.-N. Fiber-Optic SPR pH Sensor Based on MMF–NCF–MMF Structure and Self-Assembled Nanofilm. *IEEE Trans. Instrum. Meas.* **2021**, *70*, 9502509.
3. Hoa, X.D.; Kirk, A.G.; Tabrizian, M. Towards integrated and sensitive surface plasmon resonance biosensors: A review of recent progress. *Biosens. Bioelectron.* **2007**, *23*, 151–160.
4. Cennamo, N.; Saitta, L.; Tosto, C.; Arcadio, F.; Zeni, L.; Fragalá, M.E.; Cicala, G. Microstructured Surface Plasmon Resonance Sensor Based on Inkjet 3D Printing Using Photocurable Resins with Tailored Refractive Index. *Polymers* **2021**, *13*, 2518.
5. Arcadio, F.; Marzano, C.; Del Prete, D.; Zeni, L.; Cennamo, N. Analysis of Plasmonic Sensors Performance Realized by Exploiting Different UV-Cured Optical Adhesives Combined with Plastic Optical Fibers. *Sensors* **2023**, *23*, 6182.
6. Cennamo, N.; Massarotti, D.; Conte, L.; Zeni, L. Low Cost Sensors Based on SPR in a Plastic Optical Fiber for Biosensor Implementation. *Sensors* **2011**, *11*, 11752–11760.
7. Gasior, K.; Martynkien, T.; Urbanczyk, W. Effect of Constructional Parameters on the Performance of a Surface Plasmon Resonance Sensor Based on a Multimode Polymer Optical Fiber. *Appl. Opt.* **2014**, *53*, 8167.
8. Kanso, M.; Cuenot, S.; Louarn, G. Sensitivity of Optical Fiber Sensor Based on Surface Plasmon Resonance: Modeling and Experiments. *Plasmonics* **2008**, *3*, 49–57.
9. Liu, C.; Zhang, X.; Gao, Y.; Wei, Y.; Wu, P.; Su, Y.; Wu, P. Fiber SPR Refractive Index Sensor with the Variable Core Refractive Index. *Appl. Opt.* **2020**, *59*, 1323.
10. Preechaburana, P.; Gonzalez, M.C.; Suska, A.; Filippini, D. Surface Plasmon Resonance Chemical Sensing on Cell Phones. *Angew. Chem. Int. Ed.* **2012**, *51*, 11585–11588.
11. De Souza Filho, C.A.; Lima, A.M.N.; Neff, H. Smartphone based, portable optical biosensor utilizing surface plasmon resonance. In Proceedings of the IEEE International Instrumentation and Measurement Technology Conference (I2MTC) Proceedings, Montevideo, Uruguay, 12–15 May 2014.
12. Wang, Y., Liu, X., Chen, P., Tran, N.T., Zhang, J., Chia, W.S., Boujday, S., Liedberg, B. Smartphone spectrometer for colorimetric biosensing. *Analyst* **2016**, *141*, 3233–3238.
13. Hossain, M.Z.; Maragos, C.M. Gold nanoparticle-enhanced multiplexed imaging surface plasmon resonance (iSPR) detection of Fusarium mycotoxins in wheat. *Biosens. Bioelectron.* **2018**, *101*, 245–252.